Atmos. Chem. Phys. Discuss., 9, 883–903, 2009
www.atmos-chem-phys-discuss.net/9/883/2009/

Atmospheric Chemistry and Physics Discussions

This discussion paper is/has been under review for the journal *Atmospheric Chemistry and Physics (ACP)*. Please refer to the corresponding final paper in *ACP* if available.

A QBO-signal in mesospheric water vapor measurements at ALOMAR (69.29° N, 16.03° E) and in model calculations by LIMA over a solar cycle

G. R. Sonnemann[1,2], P. Hartogh[1], S. Li[1], M. Grygalashvyly[2], and U. Berger[2]

[1]Max-Planck-Institute for Solar System Research, Max-Planck-Str. 2, 37191 Katlenburg-Lindau, Germany
[2]Leibniz-Institute of Atmospheric Physics at the University Rostock in Kühlungsborn, Schloss-Str. 6, 18225 Ostseebad Kühlungsborn, Germany

Received: 4 November 2008 – Accepted: 13 November 2008 – Published: 13 January 2009

Correspondence to: M. Grygalashvyly (gryga@iap-kborn.de)

Published by Copernicus Publications on behalf of the European Geosciences Union.

Abstract

Microwave water vapor measurements between 40 and 80 km over a solar cycle (1996–2006) were carried out in high latitudes at ALOMAR (69.29° N, 16.03° E), Norway. Three larger interuptions in the winters of 1996/97 and 2005/06, and from spring 2001 to spring 2002, a few smaller interruptions of monitoring occurred during this period. The observed year-to-year variability is not directly related to the solar activity. The analysis of the observations by the Fast Fourier Transform (FFT) method revealed peaks close to two years, particularly in the upper monitoring domain. Model calculations by means of the real date model LIMA, Leibniz-Institute Middle Atmosphere model, reflect essential patterns of the water vapor variation. The FFT-analysis of the calculated water vapor mixing ratios also showed peaks of around two years. The real period of the QBO during the monitoring period ranged quite close to two years within the time interval considered, with the exception of the years 2001/02 when the period was essentially longer. Although the QBO is a phenomenon occurring in the zonal wind of the tropical stratosphere, we suppose an influence of the QBO on the water vapor distribution of the mesosphere of high latitudes controlled by transport processes. A possible link could be given by the planetary wave activity triggered by the QBO.

1 Introduction

The quasi biennial oscillation (QBO) describes how in the tropical stratosphere the zonal wind changes its direction in a rhythm of quasi two years. For instance, a west wind system prevailing approximately one year will be replaced by an east wind system. The period is, on average, somewhat larger than two years and amounts to about 28 months. The reverse starts in the upper to middle stratosphere (about 10 hPa) and progresses downward (about 100 hPa) with a speed of 1 km per month, so that it may reach the lower stratosphere when the new cycle begins in the upper stratosphere. Therefore, a certain phase of the zonal wind relates only to a distinct height range.

ACPD

9, 883–903, 2009

However, the extension of the height range of a special wind regime varies with time so that this wind direction dominates, usually when the wind reverse starts in the upper domain. The amplitude of the easterly phase is twice as large as the westerly one. During the last solar cycle, the period of the QBO amounted to almost two years for most QBO-cycles, with the exception that during 2001/02 the long-stretched tongue of an easterly wind system occurred below 30 hPa.

The middle atmospheric water vapor is controlled both by both transports and chemistry. The intra-tropical convection lifts tropospheric air through the hygropause – the cold trap for water vapor – into the stratosphere. The freeze-drying of water vapor reduces its mixing ratio from several hundred ppmv in the troposphere down to about 4 ppmv above the hygropause. Simultaneously, methane crosses this border without being subjected to the freeze-drying effect. Once in the stratosphere, methane will be oxidized to water vapor, thus enhancing its mixing ratio with increasing height. In global average, this methane oxidation is a permanent water vapor source in the middle atmosphere. As the water vapor concentration cannot permanently grow, the globally averaged water vapor flux is downward directed (Sonnemann and Körner, 2003) and enters the troposphere in middle and high latitudes together with stratospheric ozone forced by the impact of low pressure troughs (Junge, 1962; Johnson and Viezee,1981) and particularly in the winter polar vortex.

Below 70 km, the effective chemical lifetime is quite long, or it is even negative below 65 km, meaning the concentration can slightly increase rather than decrease due to an autocatalytic formation of water vapor from the H_2-reservoir (Sonnemann et al., 2005) and due to an oxidation of a small rest of methane. The effective lifetime considers both production and loss processes. The destruction of water vapor resulting in the formation of hydrogen radicals does not influence the mixing ratio as long as the hydrogen radicals return to water vapor. The mesospheric water vapor is influenced by the solar activity but dominant in a time scale of a solar cycle due to the variation of the Lyman-α radiation. A quasi-biennial oscillation of water vapor cannot directly result from the chemistry, but points rather strongly to transport processes. In the domain

ACPD
9, 883–903, 2009

under investigation, only the advective transport is relevant.

Below we briefly describe the microwave device and the LIMA model in Sect. 2.1 and 2.2, present the results in Sect. 3, and discuss the results in Sect. 4. Finally, in Sect. 5, the main findings are summarized.

2.1 Brief description of the microwave device

The microwave technique is an established tool to investigate the composition of the atmosphere with respect to certain measurable minor constituents such as water vapor or ozone. The microwave monitoring system used was described in detail by Hartogh and Hartmann (1990), Hartogh and Jarchow (1995), Seele and Hartogh (1999, 2000), Hartogh et al. (2004), Villanueva and Hartogh (2006) and Villanueva et al. (2006) among others. The ground-based radiometer uses the rotational line at 22.24 GHz for the water vapor measurements. The instrument consists of a so-called radiometer frontend and a spectrometer backend. The frontend is a heterodyne receiver detecting the 22.24 GHz water vapor line. A single side band filter filters the atmospheric signal. This filtered signal is then combined with the local oscillator signal and subsequently fed into a cooled Schottky mixer. The mixer provides a signal that is converted down, then amplified, and finally analyzed in the spectrometer backend. The vertical resolution of the water vapor retrievals depends on height and signal-to-noise ratio of the measurements and varies between 5 to 10 km, the integration time amounts to 1 day in the upper domain. The upper monitoring border is confined to 80 km. The uppermost panel is the most uncertain one and the inferred values could be somewhat underestimated in summer. To get a signal as large as possible, the elevation of the line of sight amounts to 30° and is southward directed, meaning the geographic position of the measurements in the upper mesosphere varies between about 68.04° (at 80 km, close to the discrete LIMA latitude of 68.75° N used for comparison) and 68.67° N (at 40 km altitude) and do not amount to 69.29° N – the latitude of ALOMAR. Water vapor has been measured at ALOMAR since the end of 1995, with three larger interruptions

ACPD
9, 883–903, 2009

in 1996/1997, 2001/2002, and 2005/2006, with some smaller gaps distributed over the time range of observations.

2.2 Brief description of LIMA

The abbreviation LIMA of the GCM stands for Leibniz-Institute Middle Atmosphere model. A comprehensive description of the dynamical part of the model was given in Berger (2008). The chemistry transport model of LIMA was introduced by Sonnemann et al. (2006). The model LIMA is based on the older versions of COMMA-IAP (Cologne Model of the Middle Atmosphere of the Institute of Atmospheric Physics, see also Sonnemann et al. (2005) and the references therein). LIMA is a coupled model of both dynamics and chemistry. It is a fully nonlinear, global, three-dimensional Eulerian grid point model extending from 0 to approximately 150 km with a vertical resolution of about 1.1 km. The dynamic model has a completely new architecture employing simplex or three-angled reduced Gaussian coordinates in the horizontal planes. The model has 41 804 horizontal grid points and a mesh size of approximately 110 km, advantageous for the considerations of the propagation of gravity waves and the avoidance of the so-called pole singularities. The main difference between LIMA and its predecessor COMMA-IAP is that COMMA-IAP calculates climatological averages, whereas LIMA employs real tropospheric and lower stratospheric temperature and horizontal wind data up to 35 km altitude from assimilation of ECMWF/ERA-40 (European Center for Medium Weather Forecast/Re-analysis Version 40) data. For the years before 2001, the model assimilates the ERA-40 data set (Uppala et al., 2005), and since 2002 we have used the operational data set of ECMWF. The atmospheric variability, including signals of planetary and gravity waves and of the QBO within the domain below 35 km, penetrates into the mesosphere/lower thermosphere (MLT-region) and results in a pronounced internal variability in the upper atmosphere. Additionally, we apply for the calculations real data of the Lyman-alpha flux according to Woods et al. (2000) (data available at: ftp://laspftp.colorado.edu/pub/SEE_Data/composite_lya/composite_lya.dat). In

ACPD
9, 883–903, 2009

this way, the model is able to calculate the propagation of planetary waves, and consequently it can create sudden stratospheric warming events as shown in Sonnemann et al. (2006).

The chemistry transport model (CTM) takes three modules into calculations using the operator splitting method: the chemistry, the transport, and the radiation module. The CTM employs the dynamical fields of the temperature, the wind components, and the pressure from the dynamical model. It also takes into consideration the advective transport and both the turbulent and molecular diffusion. We have adopted an eddy diffusion profile according to Lübken (1997), which does not depend on latitude and time. This is certainly restriction-influencing, particularly the mesopause region but less the mesosphere itself. However, spatio-temporal eddy diffusion profiles to employ for the chemical transport are not yet available. We use a new transport scheme according to Walcek (2000) marked by a considerably reduced numerical diffusion. The chemical module is based on a commonly used family concept (Shimazaki, 1985) considering the odd hydrogen (H, OH, HO_2), the odd oxygen (O, $O(^1D)$, O_3), and the odd nitrogen (NO, NO_2, $N(^4S)$, $N(^2D)$) families.

3 Results

Figure 1 shows an outline of the seven-day sliding average of the water vapor measurements at ALOMAR, (69.29° N, 16.03° E), Norway, from the end of 1995 until 2006. Apart from three interruptions in the winters of 1996/97 and 2005/06, and from spring 2001 to spring 2002 several small gapes of measurements occurred during this time interval. The figure displays the typical patterns of the water vapor distribution in high latitudes. The annual variations are clearly recognizable. In winter, the impact of sudden stratospheric warmings (SSWs) enhancing the water vapor mixing ratio and in summer a weak double peak of the mixing ratio can be seen. A cursory inspection by eyes shows a tendency of alternating water vapor concentrations of the summery maximum at the stratopause.

ACPD
9, 883–903, 2009

Figure 2 exhibits the same state of affairs for the LIMA calculations (68.75° N, 16.0° E) close to the ALOMAR position. A certain year-to-year variability is recognizable, but not a distinct alternating behavior. During winter, SSWs clearly impact the water vapor distribution and during summer a water vapor double maximum in altitude also occurs.

Figure 3 depicts the results of a FFT analysis. The upper penal displays results of the measurements and the lower one of the calculations at 80, 70, 60, and 50 km, respectively. The dominant peak is, as expected, that of the annual variation. The semiannual variation is more pronounced in the analysis of the calculations than in the observations. At 50 and 60 km, the semiannual variation can be neglected in the observations. The semiannual peak mainly results from the statistics of the influence of the SSWs in winter; therefore, the reason of the semiannual variation in high latitudes is different from the one in low latitudes (Körner and Sonnemann, 2000; Lossow et al., 2008). A broad peak of the amplitude occurs at about two years. This peak is more dominant in the observations and becomes clearer with increasing height. For the lower panels (50 and 60 km), a second peak occurs at less than three years, which is even larger than the two-year peak. In the calculations, this peak is absent and the two-year peak is less pronounced.

Figure 4 displays the results of the FFT analysis of LIMA data if using the absolute amounts of the zonal wind component. If not using the absolute amounts but the calculated values, the annual components strongly dominate due to the annual wind reverse and mask the two-year component, whereas now the semiannual component becomes more prominent, particularly in the upper domain, and the annual component is reduced. The figure depicts besides periods of less than one year a relatively clear separated peak of somewhat larger than two years for all panels considered. This two-year peak of the absolute amounts indicates that the dynamics varies with a period of about two years. A similar result one gets for the vertical wind, as Fig. 5 makes clear. All dynamical parameters possess a small peak near two years.

Figure 6a shows the correlation diagram for the water vapor measurements for July/August using the diurnal values if comparing the water vapor mixing ratio

at 70 km with that at 50 km. The correlation analysis (R=0.350) revealed that the water vapor at 70 km depends on that at 50 km according to the formula $[H_2O]_{70}=4.000+0.378[H_2O]_{50}$. The slight positive correlation indicates that a variation of the humidity affects the whole mesosphere, but a variation of the humidity at 50 km by 1 ppmv entails only a variation of the respective value at 70 km by 0.378 ppmv. Both quantities have the same value for $[H_2O]_{50=70}=4.0/(1-0.378)=6.431$ ppmv. $[H_2O]_{50}$ is greater than the value it follows $[H_2O]_{70}<[H_2O]_{50}$ (the normal case) and vice versa. One gets the same assertion if considering the gradient of the water vapor mixing ratio. As Fig. 6b demonstrates, correlating the diurnal mean water vapor mixing ratios at 50 km for July/August again with the respective difference of the values between 50 and 70 km, this difference becomes larger in years of high values with mixing ratios at 50 km, meaning the mixing ratio decreases faster with altitude in this case. The difference can also become negative, as the figure makes clear. For consideration of the gradient, the dependence can be written as: $[H_2O]_{50}-[H_2O]_{70}=-4.0+0.622[H_2O]_{50}$. The correlation coefficient is higher with R=0.524. This result notifies that the vertical transport in the mesosphere slows down in periods of larger mixing ratios at the stratopause, whereas relatively small values at the stratopause indicate a stronger upward transport enhancing the mixing ratios and lessening the values at 50 km. The second formula converted into the form of the first leads to the same dependence, as exhibited above.

4 Discussion

The LIMA model assimilates real data up to 35 km, but the CTM uses identical lower boundaries for all species, particularly for water vapor and methane from year to year. It is unable to model the water vapor exchange processes between the troposphere and stratosphere and does not consider the freeze-drying of water vapor at the hygropause. In other words, the long-term variations of the calculated data in the mesosphere with periods of about two years must result from the variation of the dynamics controlled

by the assimilated data. The stronger response of the observations concerning the QBO impact compared with the calculations may hint to an influence of the exchange processes between troposphere and stratosphere. A change of the Brewer-Dobson circulation, which also influences the water vapor distribution in the stratosphere was supposed and discussed by Randel et al. (2006) and Scherer et al. (2008). The Brewer-Dobson circulation also controls the transport of methane, which is the most important chemical source of water vapor in the middle atmosphere. In 1998, Randel et al. reported QBO variations in stratospheric methane and water vapor observed by HALOE, and in 2004 Randel et al. stated that the QBO signal of stratospheric water vapor is attributable to tropical tropopause temperature changes. Lossow et al. (2008) reported a QBO signal in mesospheric water vapor in low latitudes measured by Odin/SMR, but, as they mentioned, a detailed analysis will be the subject of a future work. The influence of the QBO on ozone was investigated by a large number of groups (Kinnersley and Tung, 1999; Steinbrecht et al., 2005). Its variation is also driven by dynamics (Brewer-Dobson circulation and temperature).

The QBO is a phenomenon occurring in the tropics, but the atmospheric dynamics are globally coupled and influence, among other things, the planetary wave activity. Outside of the tropical stratosphere, different groups reported QBO signals. As early as 1980 Holton and Tan found that major stratospheric warmings occur preferentially during the easterly phase of the QBO. In a large series of papers, Labitzke and van Loon showed that the SSWs and the 11-year solar activity are connected if the SSWs are ordered according to the phase of the QBO (Labitzke, 1987, 2001, 2004; Labitzke and van Loon 2000; van Loon and Labitzke, 2000; Labitzke et al., 2006). As mentioned above, the SSWs are connected with a wind reversal or a considerable slow down of the wind in the middle atmosphere. The wintry downward transport reverses into an upward transport conveying water vapor from the lower domain into the mesosphere. This influence can explain a wintry signal of the QBO in the water vapor distribution as SSWs occur more frequently during the easterly phase of the QBO (Holton and Tan, 1980). Nevertheless, evidently, the QBO also influences the water vapor mixing ratio

ACPD
9, 883–903, 2009

in high summery latitudes.

Peña-Ortiz et al. (2006) reported a QBO modulation of the circulation in both ERA 40 and MAECHAM5 simulations. Bittner et al. (2000) and Höppner and Bittner (2007) found that the planetary wave activity at mean latitude (Wuppertal, Germany, 51° N, 7° E) is modulated by the QBO. The activity is most enhanced when the wind direction of the mean zonal wind of the QBO changes from westerly to easterly. Jakobi et al. (1997) showed that the QBO, a phenomenon of the tropical stratosphere, also influences the wind system in the mesopause region of middle latitudes. In addition, Ruzmaikin et al. (2005) discussed extratropical signatures of the QBO. These findings agree with the FFT-analysis of the absolute values of the dynamical parameters of LIMA.

The interruptions in the observations, the general decrease of water vapor after 2001 (Randel et al., 2006; Scherer et al., 2008), and the limited number of years of monitoring make it difficult to interpret the meaning of the quasi three-year signal in the lower mesosphere, as well as recognize the observations at the 50 and 60 km panels in the FFT analysis. We also must consider that a distinct phase step occurred for the QBO in 2000/01 and that in 2001/02 no measurements were carried out. The impact of the QBO on the mesospheric water vapor distribution in high latitudes is certainly different for summer and winter conditions when in the later case SSWs have a strong impact on the mesospheric water vapor distribution. Unfortunately, the interruptions were all during the winter season. In spite of these restrictions, the analyses point to a real QBO-signal in the mesospheric water vapor distribution in high Northern latitudes.

5 Summary

Water vapor measurements by means of the microwave technique were carried out at ALOMAR over a solar cycle with three larger interruptions and some smaller gaps. The FFT analysis brought evidence that the QBO also influence the mesospheric water vapor distribution in high latitudes. Their signal becomes clearer above the lower

mesosphere. Model calculations by means of the GCM LIMA showed a smaller response to the QBO. One reason for this finding could be that the model calculations use lower boundary conditions repeating from year to year. The varying exchange processes between troposphere and stratosphere are not considered in the model. A particular influence may have the Brewer-Dobson circulation controlled by the QBO. A clear quasi two-year signal revealed the FFT analysis for the absolute amounts of the dynamical components in the LIMA data; meaning that the wind strength varies, independent of their direction, in a rhythm of quasi two years, thus influencing the transport of long-lived minor constituents. Among other species, this modulation also concerns species such as water vapor and methane. Methane will be oxidized to water vapor in the middle atmosphere modulating the water vapor concentration. A consequence of an alternating vertical wind is that the main middle atmospheric maximum of the water vapor mixing ratio and its secondary maximum in height at about 70 km vary opposite. The semiannual variation seen in the Fourier spectra results mainly from the SSWs occurring with a phase shift of half a year to the main summer maximum. This signal becomes clearer with increasing height.

Acknowledgements. This work was supported by the German Research Community DFG, grants HA 3261/4-1, So 268/4-1 and CASES SPP Grant LU 1174/3-1.

References

Berger, U.: Modeling of the middle atmosphere dynamics with LIMA, J. Atmos. Sol.-Terr. Phy., 70, 1170–1200, 2008.

Bittner, M., Offermann, D., and Graef, D.: Mesopause temperature variability above midlatitudev station in Europe, J. Geophys. Res., 105, 2045–2058, 2000.

Hartogh, P. and Hartmann, G. K.: A high resolution chirp transform spectrometer for microwave measurements, Meas. Sci. Technol., 1, 592–595, 1990.

Hartogh, P. and Jarchow, C.: Ground-based detection of middle atmospheric water vapour, Global Process Monitoring and Remote Sensing of the Ocean and Sea Ice, edited by: Deering, D. W. and Gudmandsen, P., Vol. 2586, Proc. SPIE, 188–195, 1995.

Hartogh, P., Jarchow, C., Sonnemann, G. R., and Grygalashvyly, M.: On the spatiotemporal behavior of ozone within the mesosphere/mesopause region under nearly polar night conditions, J. Geophys. Res., 109, D18303, doi:10.1029/2004JD004576, 2004.

Holton, J. R. and Tan, H. C.: The influence of the equatorial Quasi Biennial Oscillation on the global circulation at 50 mb, J. Atmos. Sci., 37, 2200–2208, 1980.

Höppner, K. and Bittner, M.: Evidence for solar signals in the mesopause temperature variability?, J. Atmos. Sol.-Terr. Phy., 69, 431–438, 2007.

Jacobi, C., Schminder, R., and Kürschner, D.: Measurements of mesopause region winds over Central Europe from 1983 through 1995 at Collm, Germany, Contrib. Atmos. Phys., 70, 189–200, 1997.

Johnson, W. B. and Viezee, W.: Stratospheric ozone in the lower troposphere-1. Presentation and interpretation of aircraft measurements, Atmos. Environ., 15, 1309–1323, 1981.

Junge, C. E.: Global ozone budget and exchange between stratosphere and troposphere, Tellus, 14, 363–377, 1962.

Kinnerley, J. S. and Tung, K. T.: Mechanisms for the extratrpical QBO in circulation and ozone, J. Atmos. Sci., 56, 1942–1962, 1999.

Körner, U. and Sonnemann, G. R.: Global three-dimensional modelling of the water vapour concentration of the mesosphere-mesopause region and implications with respect to the noctilucent cloud region, J. Geophys. Res., 106, 9639–9651, 2001.

Labitzke, K.: Sunspots, the QBO, and stratospheric temperatures in the north polar region, Geophys. Res. Lett., 14, 535–537, 1987.

Labitzke, K. and van Loon, H.: The QBO effect on the solar signal in the global stratosphere in

winter of the Northern Hemisphere, J. Atmos. Sol.-Terr. Phy., 62, 621–628, 2000.
Labitzke, K.: The global signal of the 11-year sunspot cycle in the stratosphere: differences between solar maxima and minima, Meteorol. Z., 10, 901–908, 2001.
Labitzke, K.: On the signal of the 11-year sunspot cycle in the stratosphere over the Antarctic and its modulation by the Quasi-Biennial Oscillation (QBO), Meteorol. Z., 13(4), 263–270, 2004.
Labitzke, K., Kunze, M., and Brönnimann, S.: Sunspots, the QBO, and the stratosphere in the North Polar region – 20 years later, Meteorol. Z., 15(3), 355–363, 2006.
Lossow, S., Urban, J., Gumbel, J., Eriksson, P., and Murtagh, D.: Observations of the mesospheric semi-annual oscillation (MSAO) in water vapour by Odin/SMR, Atmos. Chem. Phys., 8, 6527–6540, 2008, http://www.atmos-chem-phys.net/8/6527/2008/.
Lübken, F.-J.: Seasonal variation of turbulent energy dissipation rates at high latitudes as determined by in situ measurements of neutral density fluctuations, J. Geophys. Res., 102, 13 441–13 445, 1997.
Peña-Ortiz, C., Ribera, P., Giorgetta, M., and Garcia-Herrera, R.: QBO modulation of the high latitude circulation in ERA40 and MAECHAM5 simulations, Geophys. Res. Abstr., 8, 08811, 2006.
Randel, W. J., Wu, F., Russell III, J. M., Roche, A., and Waters, J. W.: Seasonal cycles and QBO variations in stratospheric CH and HO observed by UARS HALOE data, J. Atmos. Sci., 55, 163–185, 1998.
Randel, W. J., Wu, F., Oldmans, S. M., Roselof, K., and Nedoluha, G. E.: Interannual changes of stratospheric water vapour and correlations with tropical tropopause temperatures, J. Atmos. Sci., 61, 2133–2148, 2004.
Randel, W. J., Wu, F., Vömel, H., Nedoluha, G. E., and Forster, P.: Decreases in stratospheric water vapor after 2001: Links to changes in the tropical tropopause and the Brewer-Dobson circulation, J. Geophys. Res., 111, D12312, doi:10.1029/2005JD006744, 2006.
Ruzmaikin, A., Feynman, J., Jiang, X., and Yung, Y. L.: Extratropical signature of the quasi biennial oscillation, J. Geophys. Res., 110, D11111, 2005.
Scherer, M., Vömel, H., Fueglistaler, S., Oltmans, S. J., and Staehelin, J.: Trends and variability of midlatitude stratospheric water vapour deduced from the re-evaluated Boulder balloon series and HALOE, Atmos. Chem. Phys., 8, 1391–1402, 2008, http://www.atmos-chem-phys.net/8/1391/2008/.

Seele, C. and Hartogh, P.: Water vapor of the polar middle atmosphere: Annual variation and summer mesosphere conditions as observed by ground-based microwave spectroscopy, Geophys. Res. Lett., 26(11), 1517–1520, 1999.
Seele, C. and Hartogh, P.: A case study on middle atmospheric water vapor transport during the February 1998 stratospheric warming, Geophys. Res. Lett., 27(20), 3309–3312, 2000.
Shimazaki, T.: Minor Constituents in the Middle Atmosphere, D. Reidel, Norwell, Mass., 1985.
Sonnemann, G. R. and Körner, U.: The total hydrogen mixing anomaly (THYMRA) around the mesopause region, J. Geophys. Res., 108, 4692, doi:10.1029/2002JD003015, 2003.
Sonnemann, G. R., Grygalashvyly, M., and Berger, U.: Autocatalytic water vapor production as a source of large mixing ratios within the middle to upper mesosphere, J. Geophys. Res., 110, D15303, doi:10.1029/2004JD005593, 2005.
Sonnemann, G. R., Grygalashvyly, M., and Berger, U.: Impact of stratospheric warming event in January 2001 on the minor constituents in the MLT region calculated on the basis of a new 3-D-model LIMA of the dynamics and chemistry of the middle atmosphere, J. Atmos. Sol.-Terr. Phy., 68, 2012–2025, 2006.
Steinbrecht, H., Haßler, B., Brühl, C., Dameris, M., Giorgetta, M. A., Grewe, V., Manzini, E., Matthes, S., Schnadt, C., Steil, B., and Winkler, P.: Interannual patterns of total ozone and temperature in observations and model simulations, Atmos. Chem. Phys., 6, 349–374, 2006, http://www.atmos-chem-phys.net/6/349/2006/.
Uppala, S. M., Kallberg, P. W., Simmons, A. J., Andrae, U., da Costa Bechtold, V., Fiorino, M., Gibson, J. K., Haseler, J., Hernandez, A., Kelly, G. A., Li, X., Onogi, K., Saarinen, S., Sokka, N., Allan, R. P., Andersson, E., Arpe, K., Balmaseda, M. A., Beljaars, A. C. M., van de Berg, L., Bidlot, J., Bormann, N., Caires, S., Chevallier, F., Dethof, A., Dragosavac, M., Fisher, M., Fuentes, M., Hagemann, S., Holm, E., Hoskins, B. J., Isaksen, L., Janssen, P. A. E. M., Jenne, R., McNally, A. P., Mahfouf, J.-F., Morcrette, J.-J., Rayner, N. A., Saunders, R. W., Simon, P., Sterl, A., Trenberth, K. E., Untch, A., Vasiljevic, D., Viterbo, P., and Woollen, J.: The ERA-40 re-analysis, Q. J. Roy. Meteor. Soc., 131, 2961–3012, 2005.
van Loon, H. and Labitzke, K.: The influence of the 11-year solar cycle on the stratosphere below 30 km: a review, Space Sci. Rev., 94, 259–278, 2000.
Villanueva, G. and Hartogh, P.: The high resolution chirp transform spectrometer for the SOFIA-GREAT instrument, Exp. Astron., 18, 77–91, doi:10.1007/s10686-005-9004-3, 2006.
Villanueva, G. L., Hartogh, P., and Reindl, L.: A digital dispersive matching network for SAW devices in chirp transform spectrometers, IEEE Trans. Microw. Theory Tech., 54(4), 1415–

1424, 2006.
Walcek, C. J.: Minor flux adjustment near mixing ratio extremes for simplified yet highly accurate monotonic calculation of tracer advection, J. Geophys. Res., 105, 9335–9348, 2000.
Woods, T. N., Tobiska, W. K., Rottman, G. J., and Worden, J. R.: Improved solar Lyman ∀ irradiance modeling from 1947 through 1999 based on UARS observations, J. Geophys. Res., 105, 27 195–27 215, 2000.

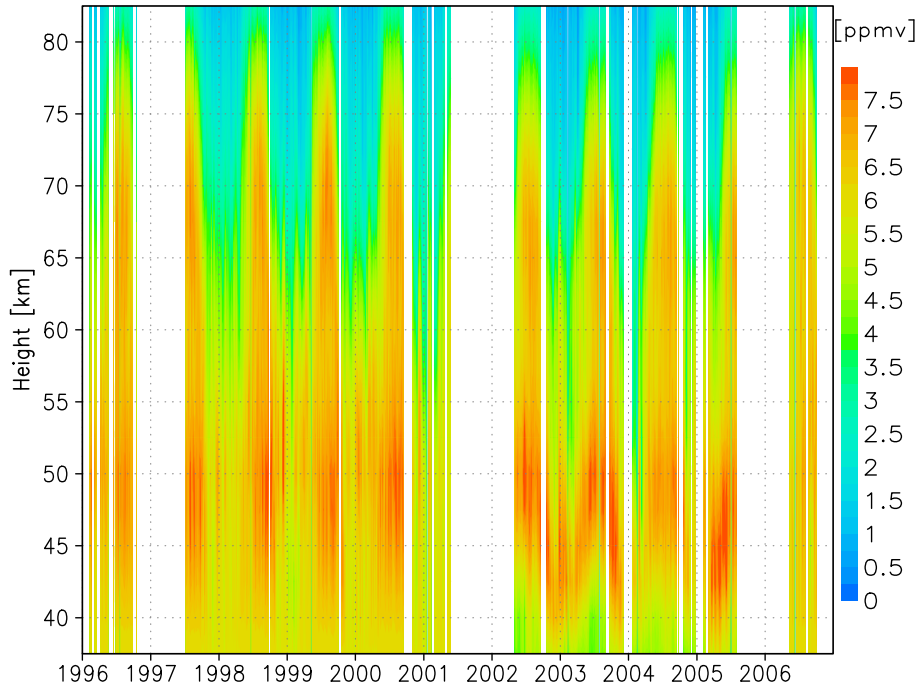

Fig. 1. Outline of the seven-day sliding average of the water vapor measurements at ALOMAR, (69.29° N, 16.03° E), Norway, from the end of 1995 until 2006.

ACPD
9, 883–903, 2009

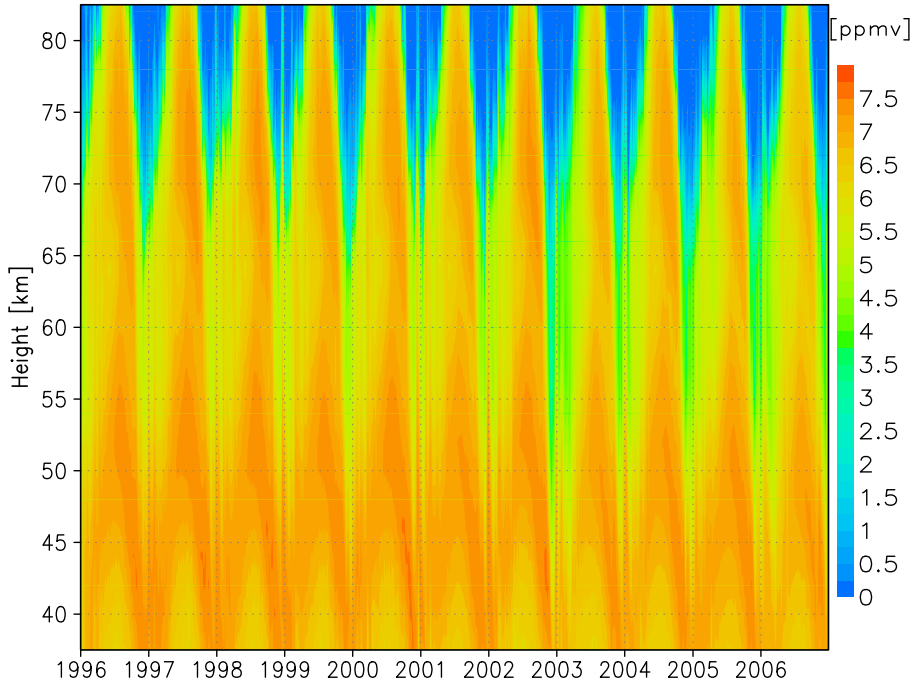

Fig. 2. Same state of affairs as shown in Fig. 1 but for the LIMA calculations at (68.75° N, 16.0° E).

ACPD
9, 883–903, 2009

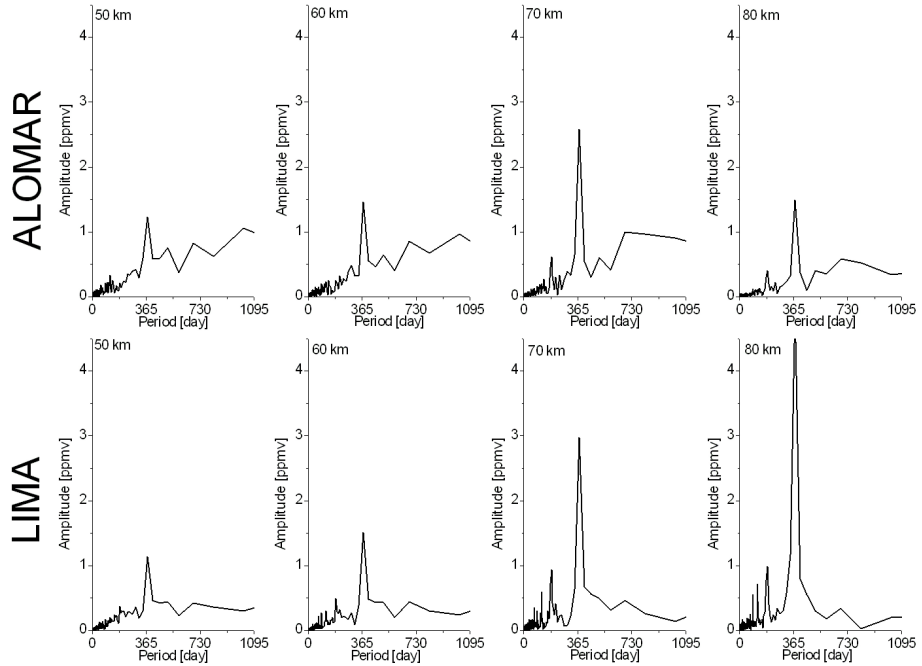

Fig. 3. FFT analysis of the ALOMAR observations (upper panel) and LIMA calculations (lower panel) at different heights.

ACPD
9, 883–903, 2009

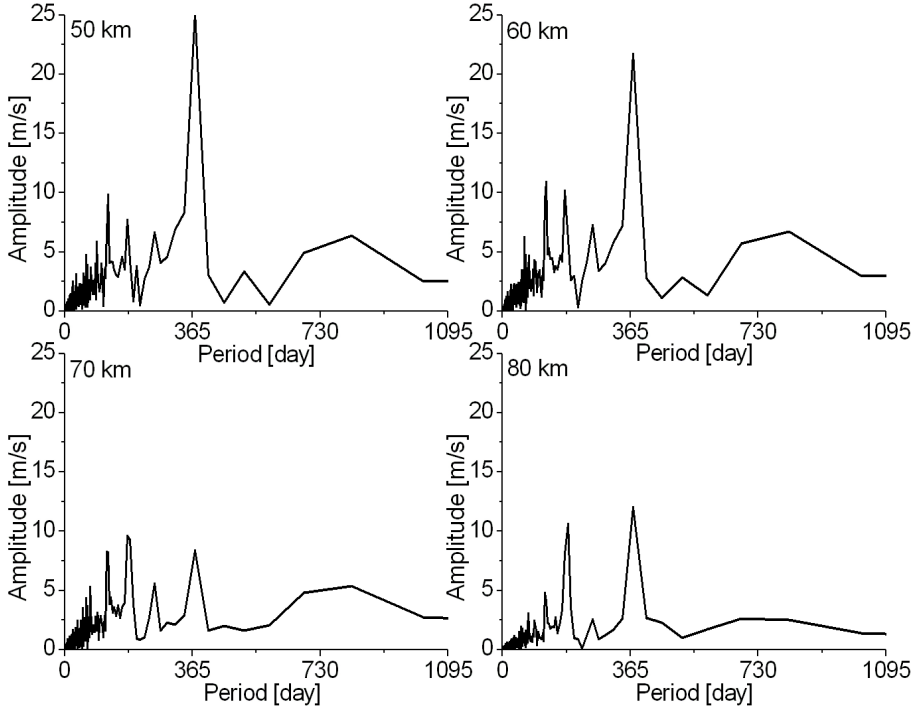

Fig. 4. FFT analysis of the LIMA data if using the absolute amounts of the zonal wind component.

ACPD
9, 883–903, 2009

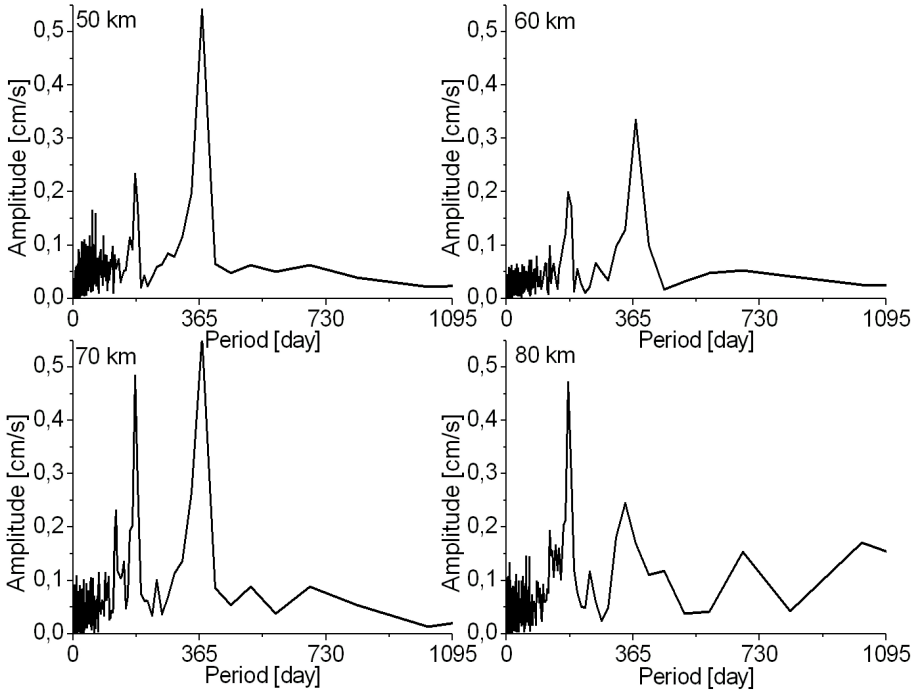

Fig. 5. Same state of affairs as shown in Fig. 4 but for the vertical wind.

ACPD
9, 883–903, 2009

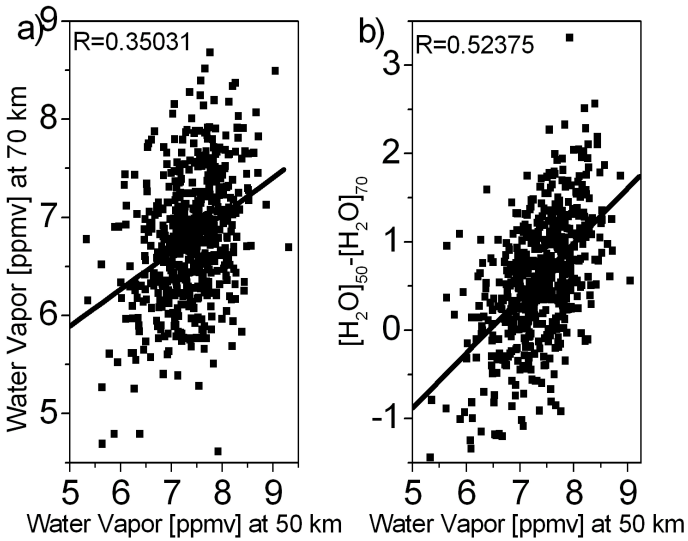

Fig. 6. (a) Correlation diagram for the water vapor measurements for July/August if comparing the diurnal water vapor mixing ratios at 70 km with those at 50 km. **(b)** Same state of affairs as shown in Fig. 6a but for the correlation between the difference of the water vapor mixing ratio between 50 km and 70 km (gradient) and that value at 50 km.

ACPD
9, 883–903, 2009